Transthyretin Amyloidosis:

Proteolytic cleavage accelerates G53A TTR aggregation

by

Jenette Arreola

May, 2020

Director of Thesis: Kwang Hun Lim

Major Department: Chemistry

The proteolytic cleavage of the peptide bond Lys48-Thr49 of the CD loop in TTR pathological mutants S52P and E51_S52dup was previously demonstrated to promote aggregation as a result of tetrameric structure destabilization. Type A and B fibrils were detected *in vivo*, suggesting alternative TTR misfolding and aggregation mechanisms. The main component of the fibrils was the residue 49-127 fragment. In the proceeding studies, the misfolding and aggregation of G53A TTR, whose mutation is nearby the K48-T49 peptide bond and also associated with TTR amyloidosis, was investigated in the presence and absence of proteolytic agent, trypsin. Fragmented G53A TTR misfolded and aggregated via a similar mechanism as full-length TTR, but at a faster rate. Similar morphology was exhibited by fragmented and full-length G53A TTR oligomers, as revealed by TEM images, suggesting similar aggregation pathway. G53A TTR in the presence and absence of trypsin generated similar CD and FT-IR profiles, suggesting similar transthyretin morphology during the early and late stages of amyloidosis. Aggregation kinetics was accomplished by monitoring the optical density of G53A TTR in the presence and absence of trypsin and by comparing the ThT fluorescence signal produced. The differences in TTR solubility and ThT enhancement imply G53A TTR aggregation is promoted in the presence of trypsin. Oligomeric effects on mammalian cell line, SH-SY5Y, was probed employing the MTT assay, which determined G53A TTR was more toxic to the cells in the presence of trypsin.

Transthyretin Amyloidosis:

Proteolytic cleavage accelerates G53A TTR misfolding and aggregation

A Thesis

Presented To the Faculty of the Department of Chemistry

East Carolina University

In Partial Fulfillment of the Requirements for the Degree

Master's of Science in Chemistry

by

Jenette Arreola

May, 2020

Transthyretin Amyloidosis:

Proteolytic cleavage accelerates G53A TTR misfolding and aggregation

by

Jenette Arreola

APPROVED BY:

DIRECTOR OF

THESIS: _____

Kwang Hun Lim, PhD

COMMITTEE MEMBER: _____

Colin Burns, PhD

COMMITTEE MEMBER: _____

Robert M. Hughes, PhD

COMMITTEE MEMBER: _____

Paul Hager, PhD

CHAIR OF THE DEPARTMENT

OF CHEMISTRY: _____

Andrew T. Morehead Jr., PhD

DEAN OF THE

GRADUATE SCHOOL: _____

Paul J. Gemperline, PhD

ACKNOWLEDGMENTS

I would like to thank Dr. Lim for the opportunity of performing research on amyloidogenic protein, transthyretin, in his lab. I could not have asked for a better graduate school experience. My enthusiasm for studying transthyretin gradually grew as more information was gathered by Dr. Lim's lab. After some time, I was able to put my work, along with previous literature findings, into perspective, facilitating my understanding the amyloidosis enigma. Dr. Dasari helped me tremendously these past few years with sample preparation, in operating instrumentation and in understanding data generated. This work could have not been possible without his guidance, patience and support!

TABLE OF CONTENTS

LIST OF FIGURES

LIST OF ABBREVIATIONS

ALZHEIMER'S DISEASE	AD
ANION EXCHANGE CHROMATOGRAPHY	AEC
CIRCULAR DICHROISM	CD
FOURIER-TRANSFORM INFRARED SPECTROSCOPY	FT-IR
NUCLEATION-DEPENDENT POLYMERIZATION	NDP
OPTICAL DENSITY	OD
PARKINSON'S DISEASE	PD
POLYACRYLAMIDE GEL ELECTROPHORESIS	PAGE
SENILE SYSTEMIC AMYLOIDOSIS	SSA
SIZE-EXCULSION CHROMATOGRAPHY	SEC
SODIUM DODECYL SULFATE	SDS
THIOFLAVIN T	ThT
THYROXINE	T4
TRANSMISSION ELECTRON MICROSCOPY	TEM
TRANSTHYRETIN	TTR
TTR AMYLOIDOSIS	ATTR
WILD-TYPE TTR	wtTTR
3-(4, 5-DIMETHYTHIAZOL-2-YL)-2, 5-DIPHENYL TETRAZOLIUM BROMIDE	MTT

1.1 Proteins

In the recent years, studying proteins and peptides on a molecular level has been of significant interest, now possible with advances in technology.[15] For example, improvements in analytical techniques, such as mass spectrometry, has enabled the elucidation of complex protein structures, crucial for unraveling molecular mechanisms of biological functions.[30] Proteins, consisting of peptides, are responsible for executing bodily functions, involved in virtually all aspects of the maintenance of life.[25] Peptides consist of a carboxyl group, an amino group and an amino acid residue and are held together by peptide bonds[15] The unique amino acid residue chain defines a protein's native three-dimensional structure which thus determines its biological function[15,30]

The protein structure consists of four levels of organization (Figure 1.1). The distinct sequence of amino acids is known as a protein's primary structure.[15,30] The secondary structure consists of α-helices and β-sheets, shaped by the folding of a polypeptide chain.[15,30] The structures are held together by hydrogen bonding between amide hydrogens and carboxyl oxygen atoms in the peptide backbone.[15,30] The overall folding of a polypeptide chain defines the protein's tertiary structure.[15,30] Various electrostatic attractive forces, such as van der Waals forces, hydrophobic interactions, attractions between oppositely charged ionic groups, disulphide bridges and hydrogen bonds, stabilize and keep the structure chain compact.[15,30] When two or more polypeptide chains associate via electrostatic interactions, the protein consists of a quaternary structure, specific to oligomeric proteins.[15,30] Each individual polypeptide chain is now referred to as a subunit or a residue of the protein.[15,30]

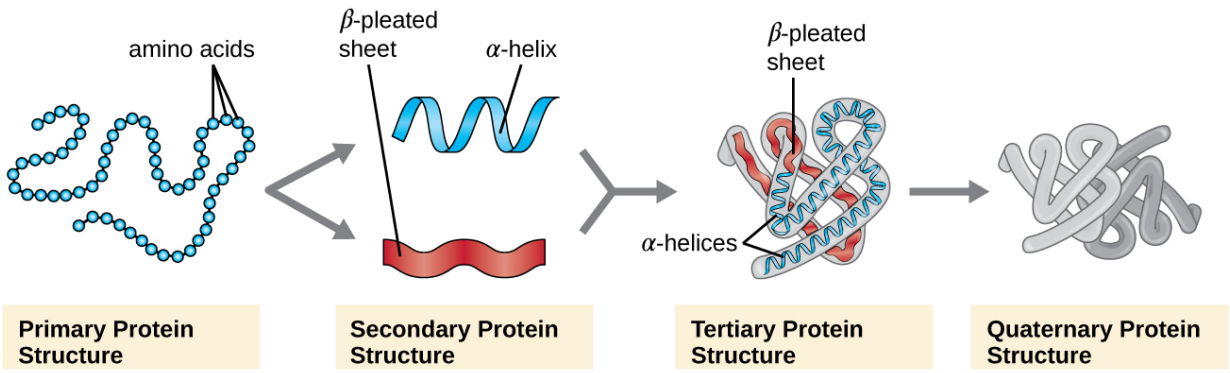

Figure 1.1 The four distinct levels of protein structure organization.[4]

The folding process is crucial as, in order to perform its biologically intended task, a protein must be structured appropriately.[23] However, proteins are prone to misfolding, failing to adopt and maintain their native conformation.[25] In this case, proteins become denatured- dysfunctional, resulting in loss of biological activity.[30] By definition, denaturation is the loss of all protein structure levels except the primary structure in which only peptide bonds remain intact.[15] Native protein destabilization and denaturation can be achieved by increasing temperature, pressure or concentration, altering pH, via oxidative stress or upon treatment with denaturants such as urea or guanidinium chloride.[15,25,30] Increasing protein concentration, for example, results in macromolecular crowding, enabling more protein interactions to occur.[20] Interactions with natural compounds, such as the metal ions Cu^{2+} or Zn^{2+}, or mutations, for instance, a site-specific replacement of a significant residue or by sequence truncating, can also trigger protein stability loss.[15,25] Furthermore, aging is accompanied with a decline in proteasomal, lysosomal and chaperone activities.[25] This affects protein homeostasis substantially as chaperons perform a multitude of cellular activities, primarily aiding proteins with native conformation

acquisition, and proteolytic degradation is fulfilled via proteasome and lysosome involvement.[25] Aging therefore comes with a decrease in protein maintenance.

1.2 Amyloidogenic Neurodegenerative Diseases

When proteins lose stability, they are susceptible to misfolding. For example, unfavorable pH changes can render the dissociation of a protein of tetramer conformation into four individual monomers. The proteins of partially unstructured conformation, misassemblies, are prone to aggregation.[25] Misfolded protein intermediates can attain toxicity and assemble into insoluble aggregates which can deposit into various organs, causing neurodegenerative diseases.[15,25,30] Generally, the protein aggregates are of amyloid structure.[29] The amyloid state occurs when disordered aggregates form long insoluble fibers, rich in β-sheets.[7,29] This conformation is known as the amyloid steric zipper (Figure 1.2).[7] Upon acquiring a β-sheet rich conformation, it is predicted that proteins will transition from having a physiological function to having a pathological one.[1]

There are approximately 30 amyloidogenic proteins associated with fatal neurological disorders.[18] As an example, Parkinson's disease (PD) is characterized by the loss of dopaminergic neurons and norepinephrinergic neurons in the brain nerves, affecting bodily movements, associated with α-synuclein Lewy bodies.[20,25,26] Alzheimer's disease (AD) is the most common neurodegenerative disorder, characterized by amyloid β and Tau protein plaques in the brain.[20,25] AD is a global health concern, primarily accounting for dementia in the elderly, resulting in an irreversible loss of intellectual abilities.[26] As of 2010, AD accounted for approximately 36 million cases worldwide, and the number is expected to reach up to 66 million by 2030.[1] In the United States alone, the disease is the 6th leading cause of death as of 2012.[1] Currently, over 20 amyloid diseases

have been discovered.[25] Unless countermeasures are found to address this health crisis, the amyloid-related deaths will continue to rise. However, why proteins misfold and evolve as pathogenic agents isn't quite understood. Predicting the correct protein folding patterns is a daunting task as the protein possesses a complex structure.[1] Thus, structural elucidation of these proteins is crucial in order to understand their pathological mechanism.

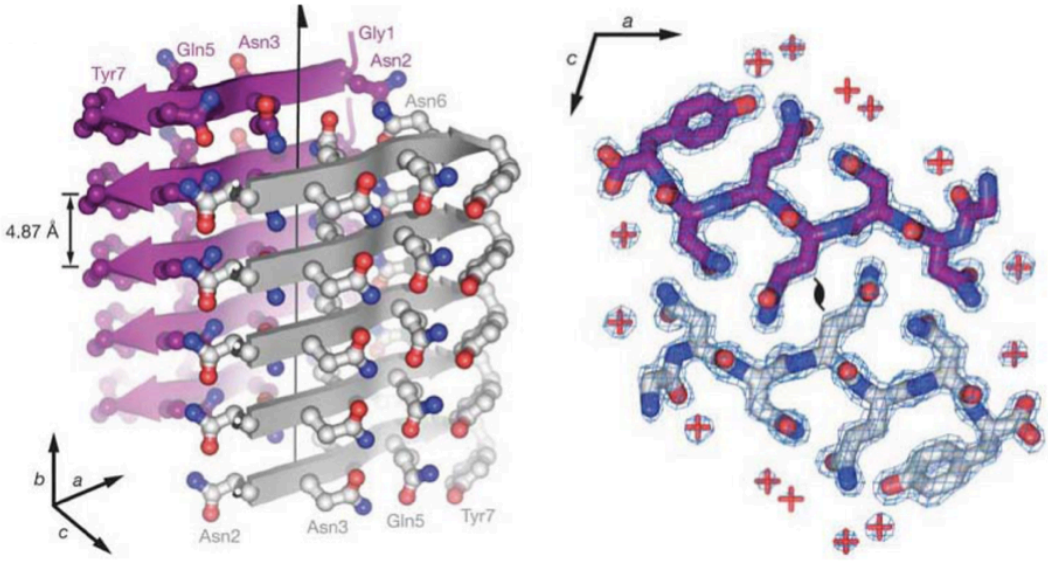

Figure 1.2 A visual of an example of the amyloid steric zipper spine consisting of 2 β-sheets, each sheet about 10 Å apart with 5 β-strands each.[7] The hydrogen bonded β-strands are about 5 Å apart from each other, and run perpendicular to the growing fibril. Protruding from each sheet are the side chains of amino acids. The carbonyl groups are symbolized by the red spheres while the amine groups are shown are blue spheres. Water molecules, indicated by the red X's, are excluded from the tight interface between the sheets, a hydrophobic region.

1.3 Transthyretin Amyloidosis

Transthyretin is one of the many globular proteins responsible for causing neurodegenerative diseases. Transthyretin (TTR) is a 55 kDa homotetrameric protein, comprised of four identical subunits, each consisting of 127 amino acid residues.[18,26] Each monomer adapts a β-sandwich fold formed by two four-stranded, antiparallel β-sheets, labeled DAGH and CBEF (Figure 1.3).[12] TTR is primarily synthesized by the liver while under 5 % is produced in the choroid plexus of the brain and the retinal pigment epithelium.[17] The tetramer serves to transport thyroxine (T4) and retinol through a ternary complex with holoretinol-binding protein.[9]

As stated previously, misfolded TTR is associated with various lethal diseases (ATTR). Sporadic ATTR is caused by wild-type TTR (wtTTR) misfolding and occurs with aging.[9] Senile systemic amyloidosis (SSA) results from wtTTR heart tissue deposits and affects up to 25 % of the population over the age of 80.[25,27] Pathogenic, point-mutations in the TTR gene can also result in tetramer destabilization, amyloid production and tissue deposits. Heart malfunction as a result of TTR variant tissue deposits is classified as cardiomyopathy.[16,25] TTR deposits in the peripheral nervous system can result in polyneuropathy or deposits in the central nervous system can cause cerebral angiopathy.[16,25] To date, over 100 single-point mutations have been identified in TTR.[3,10,11] The majority of these mutations induce disease with a much sooner age of onset than does wtTTR.[3,10,11]

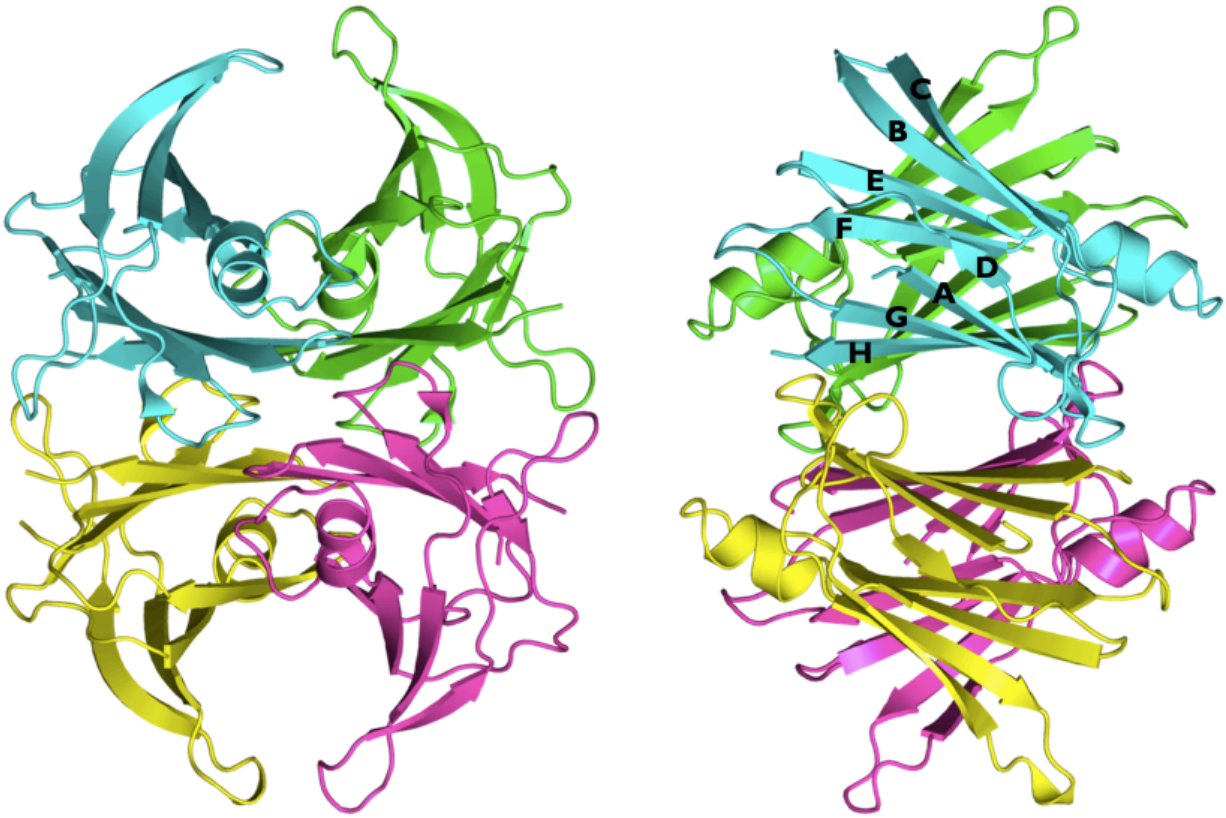

Figure 1.3 The front and side view of the crystal structure of native state transthyretin comprised of 4 identical subunits, each containing an α-helix and two antiparallel β-sheets labeled DAGH and CBEF.[24] Between the two tetramer dimers is a hydrophobic region where thyroxine binds.

The transthyretin aggregation process is initiated after full-length TTR undergoes the rate-limiting step, the dissociation of the tetramer into monomers, which then undergo partial denaturation and misassemble into aggregate structures including amyloid.[25] TTR amyloid formation and aggregation is a nucleation-dependent polymerization (NDP) reaction, also referred to as a downhill polymerization at high concentrations (Figure 1.4).[14,25] Nucleation involves the formation of a toxic, high-energy oligomeric intermediate, a nucleus, necessarily for the aggregation to become spontaneous.[13,14,25] Oligomers are non-fibrilllar aggregates or small multimeric assemblies.[8] They represent

the earliest intermediates of the amyloidogenic pathway, followed by protofibrils and mature fibrils.[8] They are typically small spherical species, lacking the enlongated, linear morphology of the proceeding two species, which are also distinguishable.[8] Protofibrils lack the high-order cross-β-structure of mature amyloid fibrils, are thinner and shorter (diameters of 10 nm vs. 10-20 nm, lengths below 400 nm vs. micrometers) and aren't fully linear.[8] Studying the cytotoxic oligomers is a daunting task as these species are of transient nature.[8] Oligomers are kinetic intermediates, constantly ongoing polymerization.[8]

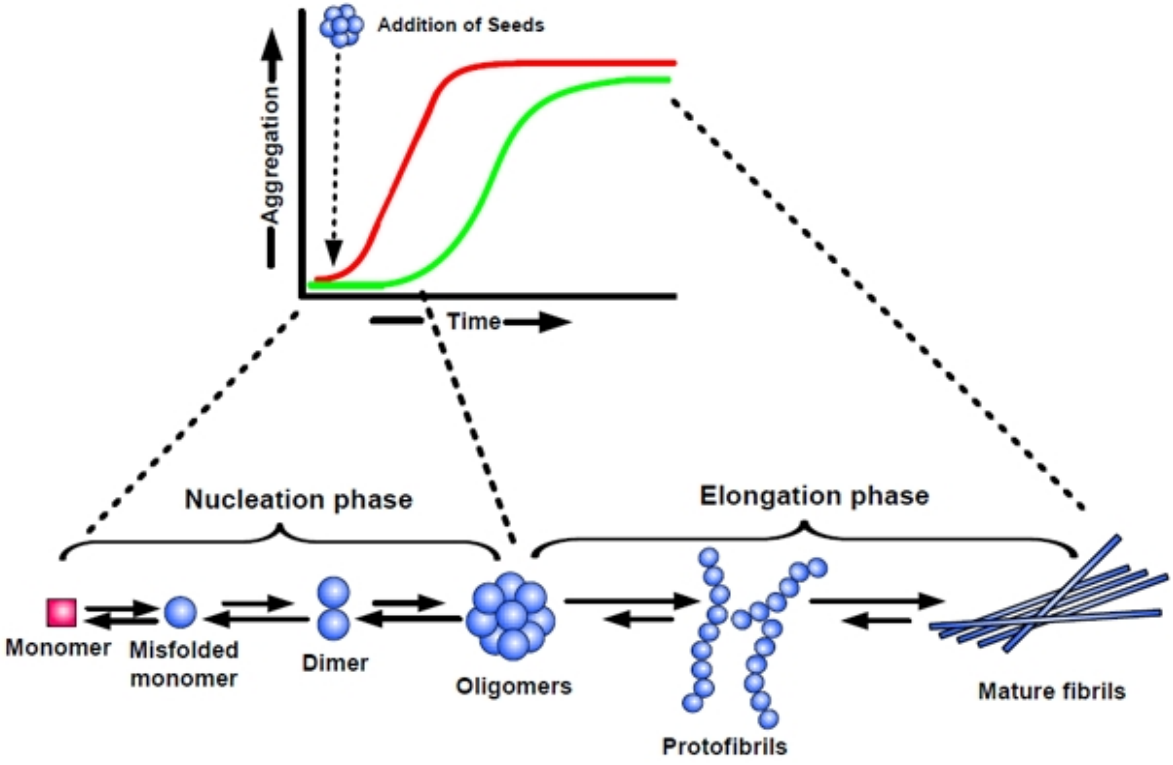

Figure 1.4 A scheme of the nucleation-dependent polymerization reaction of amyloid aggregation.[14] The nucleation phase, also known as the lag phase, is a slow process and the elongation or growth phase is rapid (green curve). The seed, a preformed amyloid species, eliminates the requirement for nucleation, resulting in rapid polymerization or aggregation (red curve).

In previous biochemical studies, fragmented TTR or type A fibrils and full-length TTR or type B fibrils were detected *in vivo*, suggesting alternative TTR misfolding and aggregation.[12,21,28] A proteolytic cleavage in the peptide bond Lys48-Thr49, found on the CD loop of TTR tetramer (see Figure 1.5), in the variants S52P and E51_S52dup resulted in significant truncated fibril formation.[12,21,28]

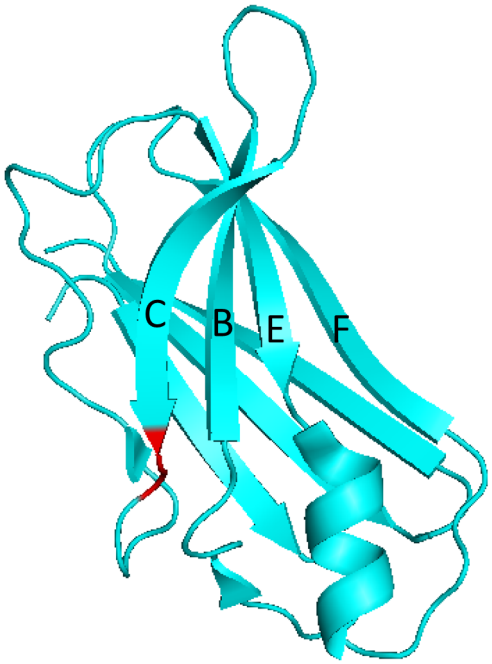

Figure 1.5 One of four TTR tetrameric subunits. On the loop amid the C and D β-strands, highlighted in red, lies the peptide-bond Lys48-Thr49.

The predominant fragment identified was the residue 49-127 C-terminal fragment.[12,21] However, the responsible protease is unknown, though the cleavage specificity suggests it is work of a trypsin-like serine protease.[21] Previously, TTR variants, V30M and L55P, were subject to digestion by trypsin and by an ubiquitous enzyme, plasmin.[22] The performance of both proteolytic agents was strikingly similar, accelerating amyloidosis.

Cleavage of the K48-T49 peptide bond was favored at physiological pH at 37 °C as a result of orbital shaking, sheer stress analogous to that experienced *in vivo* in the heart.[22] However, the molecular aggregation mechanism of cleaved TTR has yet to be determined, as well as that of full-length TTR. Different dissociation paths may be taken by full-length and fragmented TTR. There are many predictions for full-length TTR dissociation (Figure 1.6). The destabilized monomers may separate individually from the tetramer, tetramer dimers may separate at the hydrophobic region where thyroxine binds or other paths may be taken upon full-length TTR destabilization. On the other hand, the cleaved C-terminal fragment (49-127), may be individually released from the TTR tetramer, proceeding to misfold and aggregate. However, the proteolytic cleavage may destabilize the tetrameric structure of TTR, promoting monomer dissociation which will proceed to form amyloid.

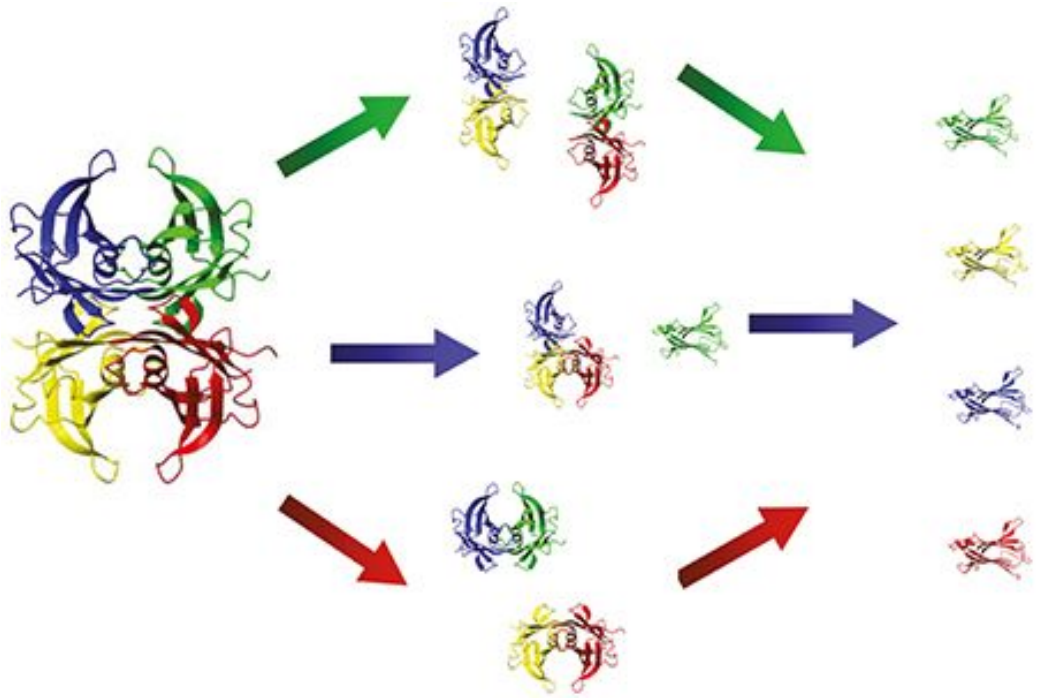

Figure 1.6 Suggested TTR dissociation pathways, resulting in amyloidosis.[2]

In hopes to provide insights to the unresolved cleaved (C-terminal fragment 49-127) and full-length transthyretin aggregation mechanisms, the misfolding and aggregation of TTR variant (G53A) in the presence and absence of trypsin was investigated. Partially misfolded proteins typically expose their hydrophobic amino acid residues, driving the NDP reaction in which three distinct aggregates are formed sequentially. Examination of the early-stage oligomeric intermediate was accomplished employing transmission electron microscopy (TEM). Circular dichroism (CD) was also employed to monitor oligomeric structural changes occurring during TTR aggregation. Studies on the continuing TTR aggregation intermediate forming, protofibril, were possible by measuring turbidity via the optical density. The fluorescence emission spectra of thioflavin T (ThT) served to confirm the presence of amyloidogenic species as ThT is known to bind to amyloid. To note any structural differences in the late-stage intermediate of aggregation, mature amyloid, Fourier-transform infrared spectroscopy (FT-IR) was utilized. The 3-(4, 5-dimethythiazol-2-yl)-2, 5-diphenyl tetrazolium bromide (MTT) assay was employed to compare the toxicity of oligomeric species produced in the presence and absence of trypsin on SH-SY5Y (human neuroblastoma) cells. The generated results from the methods employed suggest the proteolytic cleavage of the K48-T40 peptide bond accelerated the formation of cytotoxic oligomers. Similar molecular structures were observed for aggregates formed in the presence and absence of trypsin. The findings imply the cleaved C-terminal fragment (49-127), identified employing the sodium dodecyl sulfate polyacrylamide gel electrophoresis (SDS-PAGE), and full-length G53A TTR variant form amyloid via a similar misfolding and aggregation pathway.

2.1 Protein Expression, Preparation and Purification

The TTR variant, G53A, was expressed in *E. coli* (calcium competent) as follows:

1. The pMMHa plasmid encoding the G53A TTR sequence was transformed into *E. coli* BL21 (DE3) and was plated onto an LB-agar plate with carbenicillin at 37 °C. The cells were grown overnight (12 h).
2. A single colony was taken and added to 5 mL LB media supplemented with carbenicillin at 37 °C.
3. The culture was used to inoculate a 500 mL culture at 37 °C. Growth was monitored by the optical density at 600 nm (OD_{600}).
4. The final culture was induced with IPTG to over-express TTR at an OD_{600} of 0.6, and the incubator temperature was reduced to 25 °C. The flask with culture was shaken overnight (12 h).
5. The cells were harvested at an OD_{600} of 1.6-1.7 via centrifugation at 4 °C (30 min at 8000 rpm), and the collected pellets were frozen at -80 °C for at least an hour before proceeding with experiment.

To extract G53A TTR from *E. coli*, the following protocol was performed:

6. Frozen pellets were thawed for 30 min and suspended in chilled 1 M Tris, 5 M NaCl (pH 8; 100 mL buffer/L of culture
7. The solution was placed on ice and was lysed via sonication (2 sec on and 2 sec off, for 30 sec) with 2 min rest to prevent overheating. This procedure was repeated 5 times for optimal lysis.

8. The lysed cells were centrifuged at 4 °C (30 min at 8000 rpm). The supernatant was collected, and the pellet was discarded.

Following cell lysis, the collected protein solution is subject to multiple purification techniques, beginning with ammonium sulfate precipitation:

9. The collected supernatant maintained at 4 °C. Ammonium sulfate (50 %) was added slowly to the solution with rigorous stirring. When all salt was added, stirring was continued for 15 min to ensure effective precipitation of unwanted cellular proteins.
10. The solution was re-centrifuged at 4 °C (30 min at 8000 rpm).
11. The supernatant was collected and dialyzed at 4 °C against 4 L dialysis buffer (1 M Tris, 0.5 M EDTA, PMSF) for a total of 12 h.

A second purification method, anion exchange chromatography (AEC), was employed:

12. The collected desalted solution was filtered and applied to a 10- HiTrap™ Q HP column (GE Healthcare) anion exchange column equilibrated with buffer A (20 mM Tris; pH 8).
13. TTR was subject to a 5 % gradient of buffer B (20 mM Tris, 5 M NaCl; pH 8) and eluted following an NaCl wash.
14. The fractions containing TTR, as determined by the characteristic chromatographic data, were pooled.

Following AEC, size-exclusion chromatography (SEC) was utilized to remove soluble aggregates of TTR solution:

15. The pooled Q-column fractions were injected into a HiLoad^{TM} 16/60 Superdex 200 gel filtration column filled with phosphate buffer (0.2 M sodium phosphate monobasic, 0.2 sodium phosphate dibasic; pH 7).
16. Purified SEC fractions were collected.

The absorbance of purified TTR (extinction coefficient of 7.76 x 10^4 M^{-1} cm^{-1}) was measured via UV-Vis spectroscopy (280 nm) with a quartz cuvette (10 mm) to determine the concentration for proceeding studies. Phosphate buffer (10 mM, pH 7.3) was used for dilution of protein. The identity was confirmed utilizing SDS-PAGE (Figure 2.1).

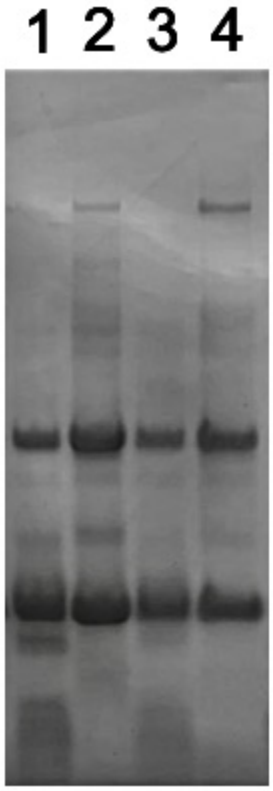

Figure 2.1 The SDS-PAGE gel results for G53A TTR at 1) 0.7 mg/mL with trypsin, 2) 0.7 mg/mL without trypsin, 3) 0.3 mg/mL with trypsin, and 4) 0.3 mg/mL without trypsin after 4 h. incubation at 37 °C with shaking. The gel verified G53A-TTR was cleaved into fragments (Lanes 1 and 3) when incubated with trypsin.

2.2 Transmission Electron Microscopy

The variant, G53A TTR (0.25 mg/mL), was incubated at physiological pH (7.3) at 37 °C with agitation (250 rpm) with and without trypsin. TEM grids were prepared after 2 h of incubation. Oligomer visualization was achieved with a Philips CM12 transmission electron microscope at 80 kV. The following protocol was used:

1. G53A was added to PBS buffer (8x dilution).
2. To previously glow-discharged formvar/carbon coated copper 400 mesh grids, 5 μL of sample was applied. The grid was securely held utilizing negative pressure tweezers.
3. The edge of each grid was gently touched to a sheet of filter paper after 30 seconds- which permitted sample adsorption to the grid surface.
4. The grids were washed with 7.5 μL 1% uranyl acetate. This addition was immediately blotted using a filter paper.
5. Negative staining was accomplished using 7.5 μL 1% uranyl acetate. The edge of the grids was touched to filter paper to remove staining solution.
6. The grids were air-dried.
7. Visualization of TTR oligomers was performed.

2.3 Optical Density

The optical density (OD_{400}) of G53A TTR (0.3 and 0.7 mg/mL, physiological conditions with agitation) in the presence and absence of trypsin was measured spectrophotometrically using a quartz cuvette (1 mm).

2.4 ThT Fluorescence

G53A TTR (0.3 and 0.7 mg/mL) was incubated with and without trypsin at 37 °C, pH 7.3 with shaking (250 rpm). The amyloidogenic precipitates were added to thioflavin:PBS (2.5 mM : 10 mM) solution 5 h after incubation. The ThT fluorescence was measured (λ_{ex} at 440 nm, λ_{em} at 485 nm) while stirring amyloid in solution.

2.5 Circular Dichroism

The following numerical bullets summarize the steps taken to set up the CD spectropolarimeter and explain how protein sample ellipticity measurements were taken:

1. The spectrometer (Jasco J-815) was purged with nitrogen gas 30 minutes before switching on the xenon light source. This step is necessary to remove oxygen from the optical system as its presence can result in detrimental effects. Oxygen absorbs in the far UV region, reducing light availability for cd measurements.[6] Furthermore, striking oxygen with UV light can result in ozone production, which can damage the instrumental optics.[6]
2. The xenon lamp source was switched on and was allowed to stabilize for 20 minutes.
3. The water bath turned on and reached 18°C prior to CD analysis.
4. The ellipticity of the blank, PBS buffer, was taken at wavelength (λ) 190-260.
5. The ellipticity of samples G53A and G53A with trypsin (0.25 mg/mL), incubated at 37 °C at a pH of 7.3 with shaking, was measured at wavelength (λ) 190-260 every 20 minutes for a period of 3 hours. An average from 10 repeated scans was calculated for each sample.
6. CD spectra were generated and analyzed.

2.6 Fourier-Transform Infrared Spectroscopy

G53A TTR (0.3 and 0.7 mg/mL) was incubated with and without trypsin at 37 °C, pH 7.3 with shaking (250 rpm). The precipitates collected (14 days incubation) were rinsed with water, air dried and the IR spectra for the amyloid were recorded (Nicolet iS50 ATR).

2.7 MTT Assay

SH-SY5Y (human neuroblastoma) cells were propagated in 225 cm^2 polystyrene cell culture flasks with vented screw caps. The cultured cells were incubated in SMEM-F12 (50:50), supplemented with 10% fetal bovine serum (FBS), at 37 °C, 5% CO_2 with humidified atmosphere. Enumeration was accomplished using a haemocytometer. The MTT assay experimental design was as follows:

1. SH-SY5Y cells (1.0×10^2 cells/well) were seeded into 96-well plate with medium and were incubated for 24 h. prior to replacing cell medium and being treated with or without trypsin and protein. This period allows cells to settle at the bottom of the microplate.
2. Cells (with duplicates) were treated with G53A TTR (0.25 mg/mL or 0.50 mg/mL) with or without trypsin at 0, 0.5 and 1 h incubation at 37 °C at a pH of 7.3 with constant agitation. Cell medium without cells was used as the blank. The cells were re-incubated for 24 h.
3. MTT (5 mg) was prepared in sterile PBS. Of this stock solution, 10 μL was added to each well containing protein with or without trypsin. Saponin (10%) was used as the positive control. The cells were re-incubated for 4 h.

4. To each well, 100 μL of prepared SDS-HCl solution was added to each well and mixed thoroughly. This addition precipitates the produced formazans.
5. The cell viability was determined 14 h post SDS-HCl addition via a spectrofluorometer (570 nm).

3.1 G53A TTR forms similar oligomeric structures in the presence and absence of trypsin

In this study, the misfolding pathway of TTR mutant G53A, which results in amyloid formation and aggregation, was examined in the presence and absence of proteolytic agent trypsin. With TEM, it was possible to compare the morphology of the cytotoxic species formed at the initiation of G53A TTR aggregation in the presence and absence of trypsin (incubated with shaking at 37 °C at pH 7.3). A TEM image of G53A TTR incubated without trypsin at 2 h is found in Figure 3.1a (Figure 3.2a, zoomed-in) where small, spherical structures are observed. In some regions of the image, small clusters of oligomers are seen, suggesting TTR aggregation has initiated. However, when G53A TTR is cleaved, aggregation is accelerated as previously demonstrated for mutants S52P and E51_S52dup. In Figure 3.1b (Figure 3.2b, zoomed-in), greater oligomeric clusters are observed, also more abundant than in the absence of trypsin, suggesting aggregation progresses more rapidly when G53A TTR is cleaved. However, the G53A TTR aggregates in the presence of trypsin are small and spherical as observed for the variant in the absence of trypsin. This implies fragmented and full-length G53A TTR may have similar misfolding and aggregation pathways.

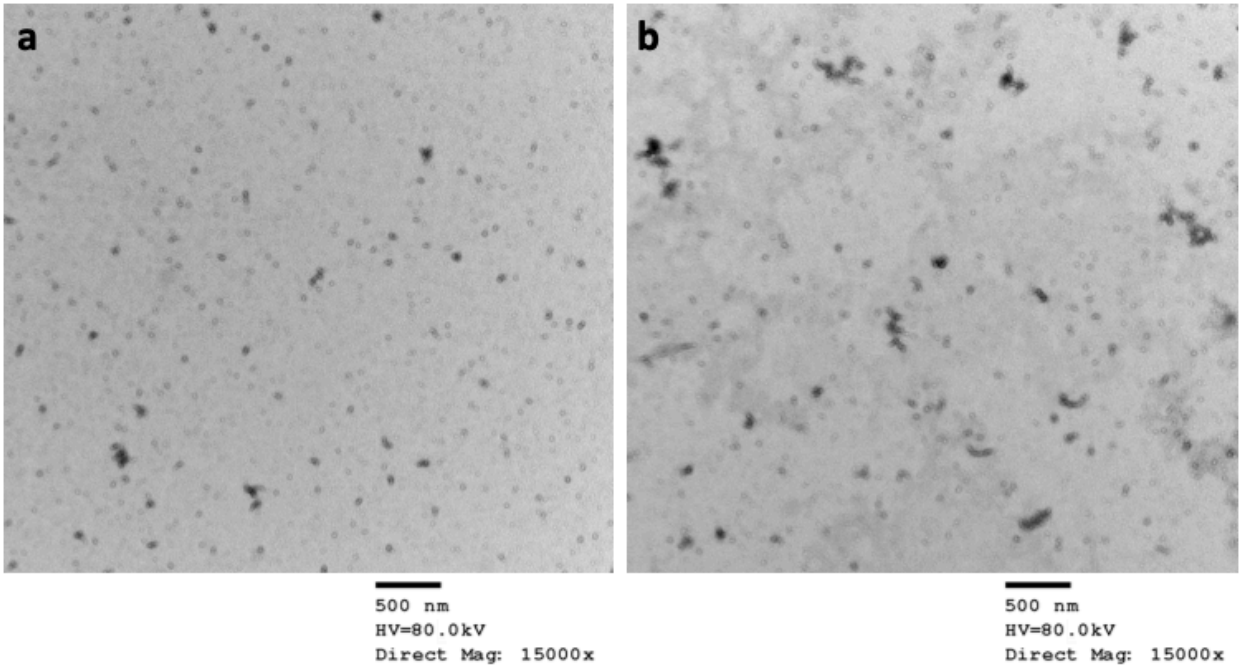

Figure 3.1 TEM images of G53A TTR (0.25 mg/mL) after 2 h incubation at physiological conditions in the absence (a) and presence (b) of trypsin.

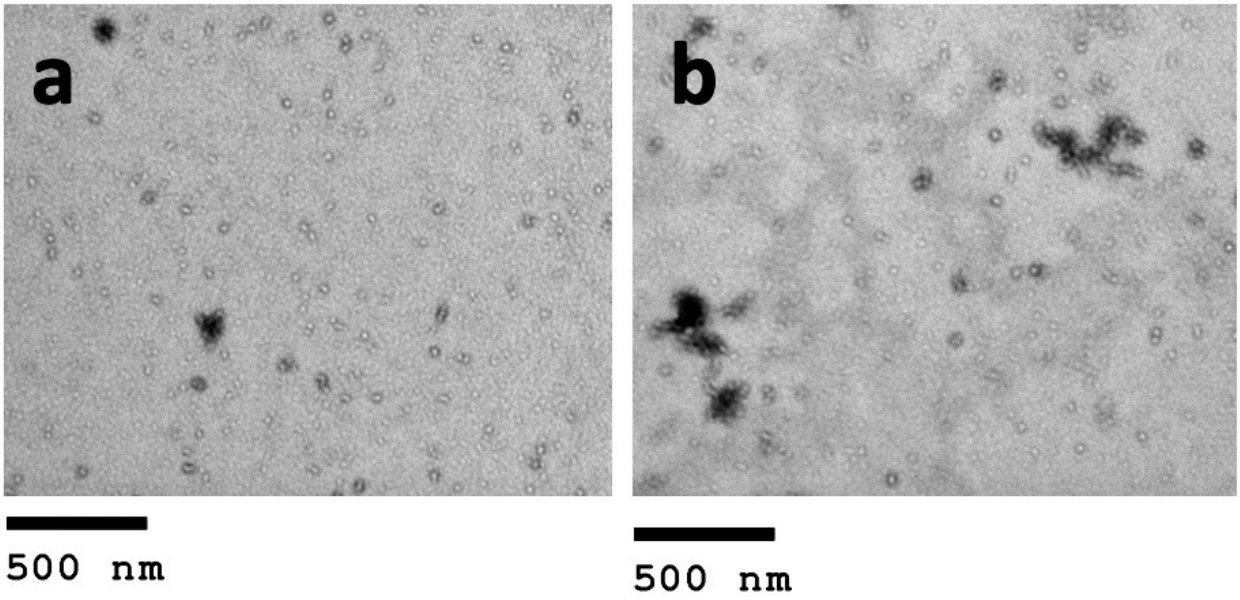

Figure 3.2 Zoomed-in TEM images of G53A TTR (0.25 mg/mL) after 2 h incubation at physiological conditions in the absence (a) and presence (b) of trypsin.

3.2 G53A TTR aggregation is accelerated upon being cleaved

In previous biochemical studies, the proteolytic cleavage of the K48-T49 peptide bond of the CD loop in TTR mutants S52P and E51_S52dup promoted aggregation. To investigate the differences in G53A TTR aggregation kinetics in the presence and absence of trypsin at physiological conditions, the optical density (OD_{400}) was monitored over a period of 32 h (Figure 3.3). G53A TTR (0.3-0.7 mg/mL) expresses low turbidity in the absence of trypsin, indicating protein solubility is high. G53A TTR (0.3 mg/mL) turbidity notably increases in the presence of trypsin as a result of insoluble protein aggregates forming in solution. However, protein aggregation is greatly promoted in the presence of trypsin at a greater TTR concentration of 0.7 mg/mL. The findings suggest G53A TTR aggregation is accelerated when subject to proteolytic cleavage.

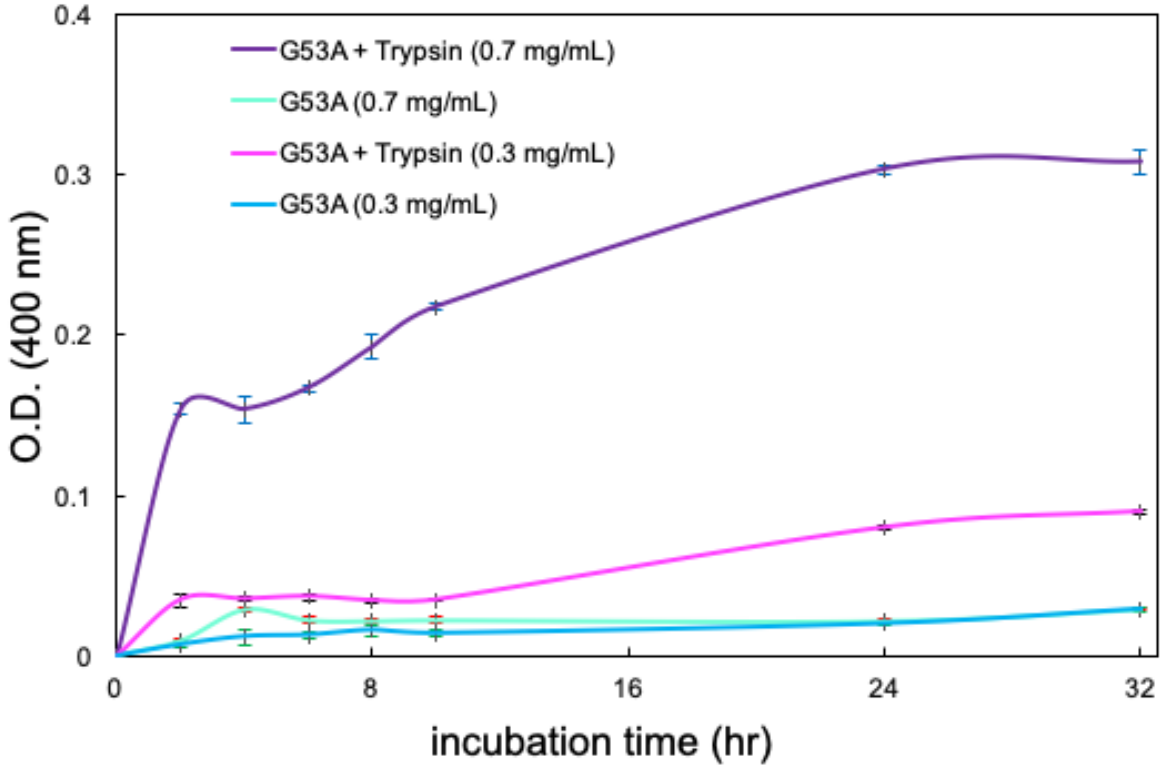

Figure 3.3 Aggregation kinetics of TTR variant G53A in the presence and absence of trypsin.

The presence of G53A TTR amyloidogenic species was confirmed via fluorescence signal produced by thioflavin T (ThT), known to bind to amyloids, giving off a strong fluorescence upon binding. Figure 3.4 displays the fluorescence emission spectra generated. In the absence of trypsin, G53A TTR (0.3-0.7 mg/mL), no significant ThT enhancement was observed, implying amyloid formation in solution was minor when G53A TTR was un-cleaved after 5 h incubation. However, in the presence of trypsin, G53A TTR (0.3 mg/mL), a greater ThT signal was observed. At a higher concentration (0.7 mg/mL), cleavage via trypsin resulted in significant ThT enhancement, indicating great formation of amyloidogenic species in solution. The findings suggest aggregation is promoted upon trypsin digestion.

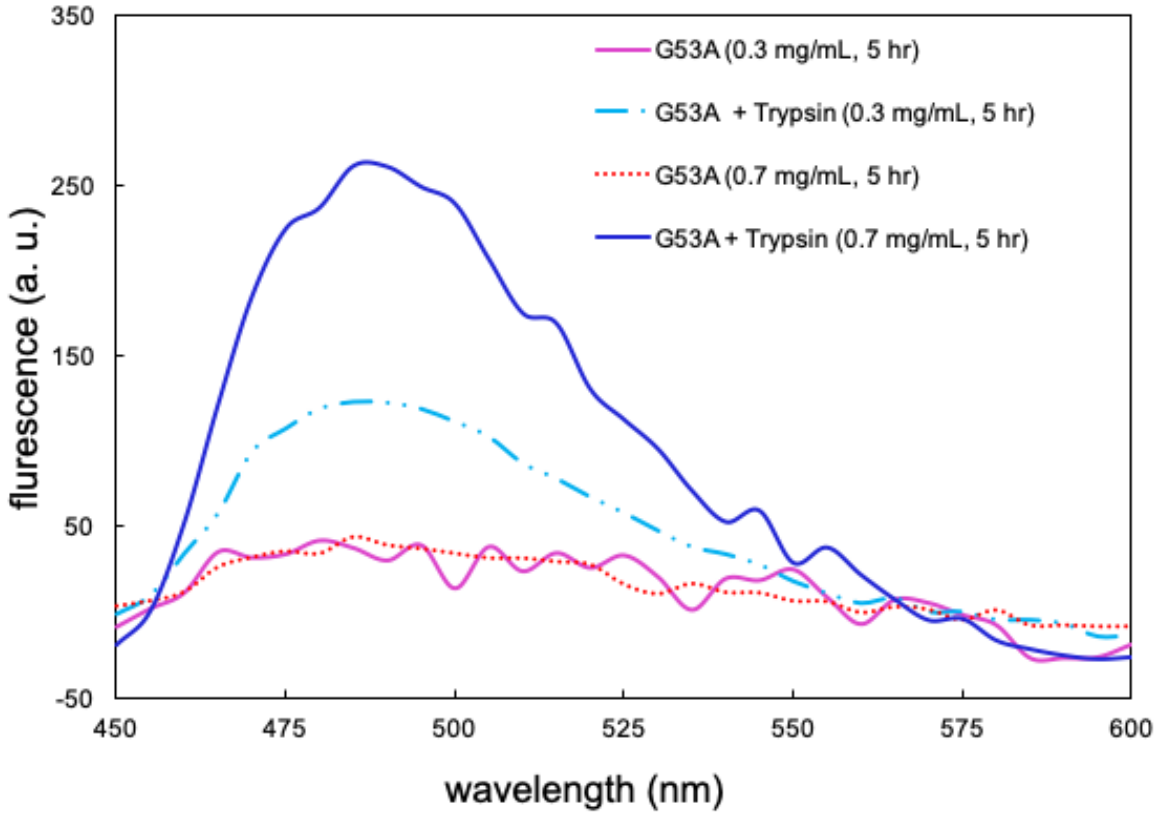

Figure 3.4 Thioflavin T (ThT) fluorescence emission spectra of G53A TTR (0.3-0.7 mg/mL) at 5 h incubation in presence and absence of trypsin at physiological conditions (λ_{ex} at 440nm, λ_{em} at 485nm).

3.3 G53A TTR exhibits a similar secondary structure when cleaved by trypsin as when un-cleaved

Circular dichroism was employed to monitor G53A TTR secondary structural changes that occur at the early stage of tetramer misfolding in the presence and absence of trypsin at physiological conditions. The generated CD spectra (Figure 3.5-3.6) reveal characteristic peaks of protein β-strands where the HT [V] is below 650 v, rendering the data reliable. At 195 nm, there is an initial maximum positive band while at 215 nm, an initial maximum negative band is observed for both G53A TTR samples. While there are minor fluctuations in the CD spectra for G53A in the absence of trypsin (Figure 3.5), more noticeable changes are observed in the presence of trypsin (Figure 3.6) at approximately the same time-frame. At 195 nm, the trypsin proteolytic cleavage of G53A TTR resulted in a diminish of peak intensity, indicating TTR undergoes greater structural changes- becomes more disordered than when TTR isn't cleaved. The negative band at 215 nm for G53A TTR in the presence of trypsin looks much like the one for G53A TTR in the absence of trypsin. The findings suggest that the cleaved TTR variant's β-structured configuration becomes slightly more disordered that than of un-cleaved TTR at the same time-point.

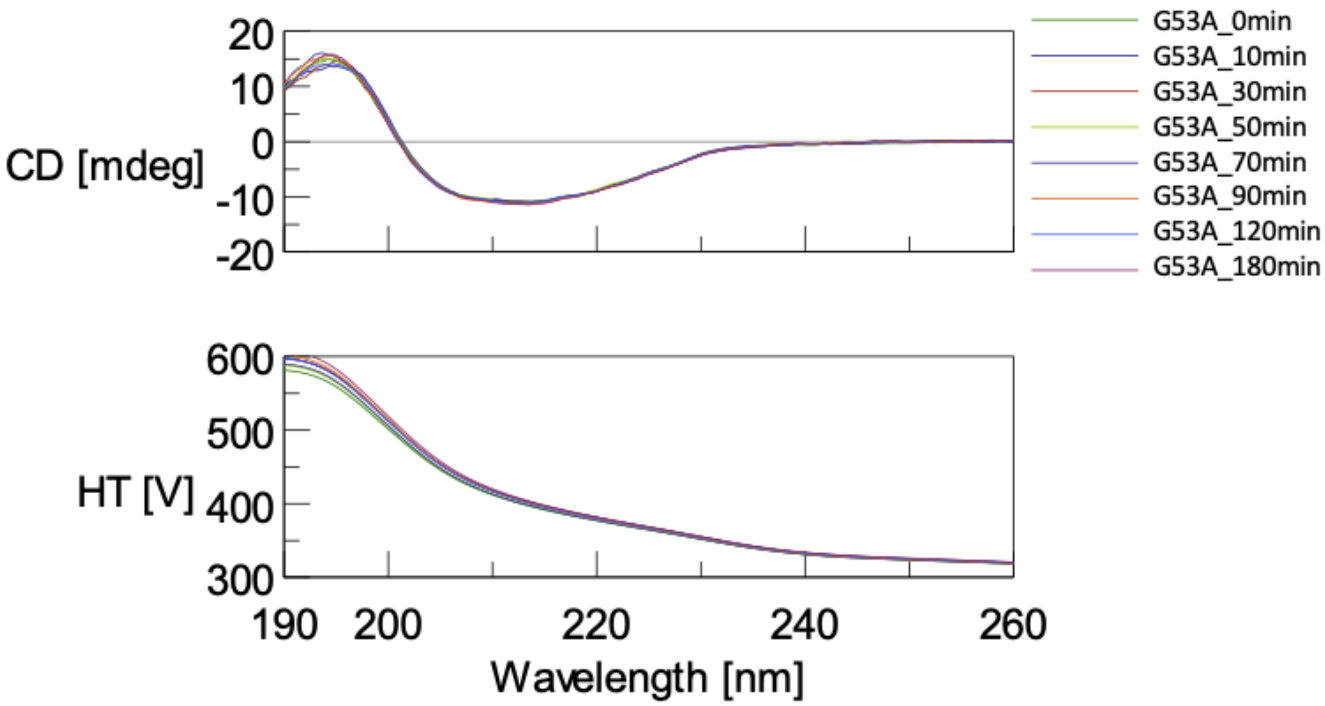

Figure 3.5 The CD spectrum of G53A-TTR (0.25 mg/mL) secondary structural changes in the absence of trypsin for a period of 180 min after incubation at physiological conditions.

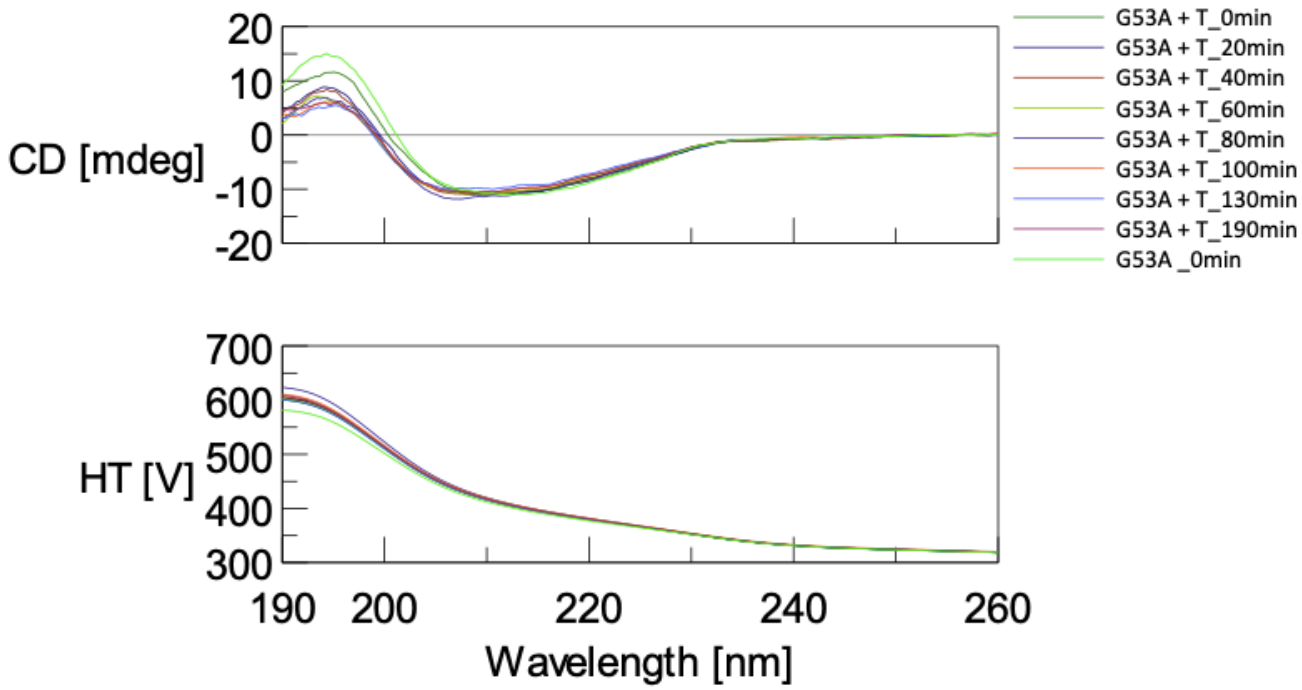

Figure 3.6 The CD spectrum of G53A-TTR (0.25 mg/mL) secondary structural changes in the presence of trypsin for a period of 190 min after incubation at physiological conditions.

G53A TTR amyloid molecules in the presence and absence of trypsin were also investigated employing FT-IR, which is sensitive to secondary structure information. Similar fragmented and full-length G53A TTR amyloid IR profiles were noticed. Nearly identical maximum absorption amide-I band was noted for both TTR samples at 1630 cm^{-1} (Figure 3.7), suggesting the variant in the presence and absence of trypsin forms amyloid with similar β-configuration. This finding is also supported as both samples in the amide-II and III regions exhibit similar absorption peaks at same wavenumbers.

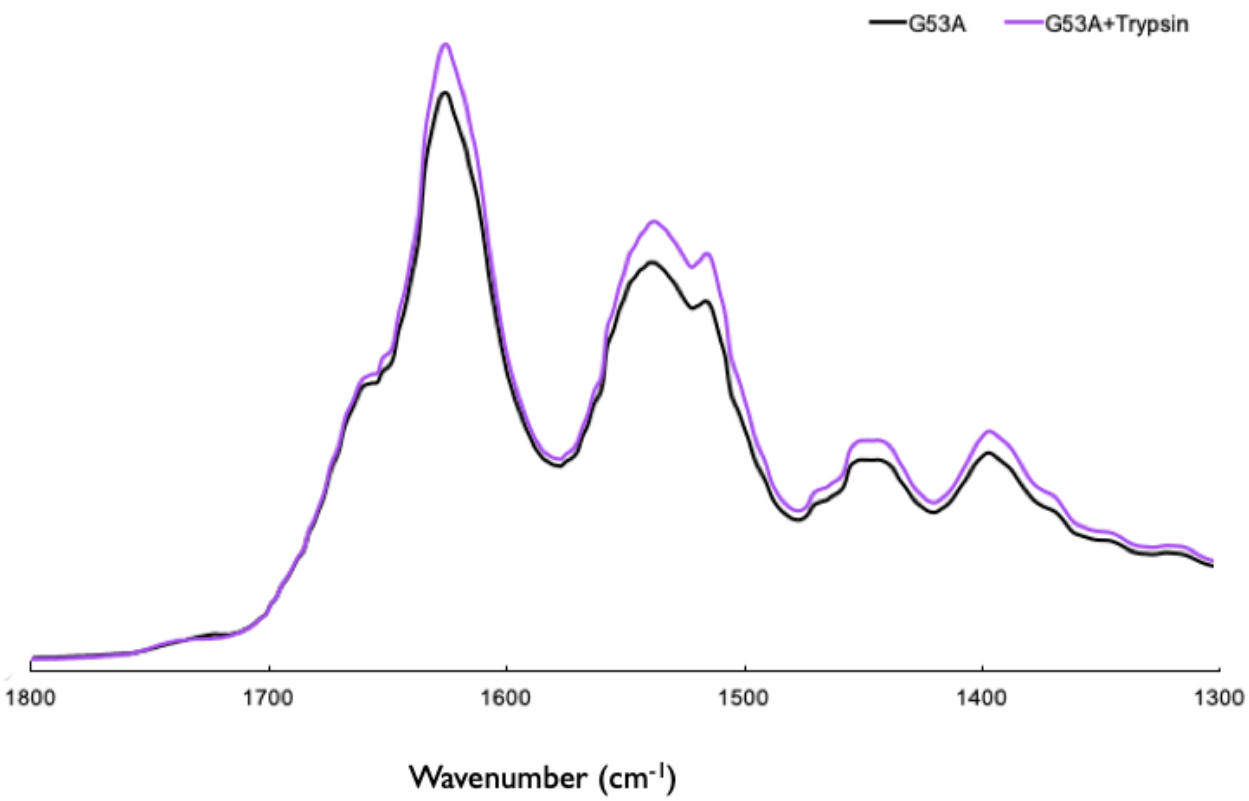

Figure 3.7 FT-IR spectra of cleaved (purple) and un-cleaved (black) TTR variant G53A amyloids collected at 14 d incubation at physiological conditions with agitation (250 rpm).

3.4 Proteolytic cleavage enhances toxicity of oligomeric species

Similar oligomeric species were formed upon fragmented and full-length G53A TTR misfolding and aggregation, visualized by TEM. It has been previously proposed the oligomeric intermediates are the real cytotoxic agents of TTR aggregation. Their toxicity was monitored over a period of 1 h in SH-SY5Y cells employing the MTT assay. Cells were treated with G53A TTR (0.25 or 0.50 mg/mL) incubated at physiological conditions in the presence or absence of trypsin. Figure 3.8 shows the cell viability results of mammalian cells treated with G53A TTR (0.25 mg/mL) in the presence and absence of trypsin. Treatment with protein alone resulted in a consistent cell viability percentage of 85 %, indicating treatment with full-length G53A TTR did not result in cell death. However, when treatment with protein was accompanied with trypsin, cell viability decreased from 100% to 60 %. The 40% cell viability loss suggests cleaved G53A TTR is more toxic than full-length TTR as a result of more oligomers being produced at the same point in time.

Figure 3.9 shows the cell viability results of mammalian cells treated with G53A TTR (0.50 mg/mL) in the presence and absence of trypsin. The same outcome was observed for G53A TTR at a higher concentration. Cleaved G53A TTR is more toxic to the cells than the un-cleaved TTR variant. However, a greater loss in percent cell viability was observed. Upon treatment with of G53A TTR (0.50 mg/mL) at 0.5 h incubation with trypsin, the cell viability decreased from 100% to 90%, and at 1.0 h incubation, cell viability decreased to 50%. The findings suggest proteolytic cleavage enhances oligomeric toxicity due to more oligomerization occurring.

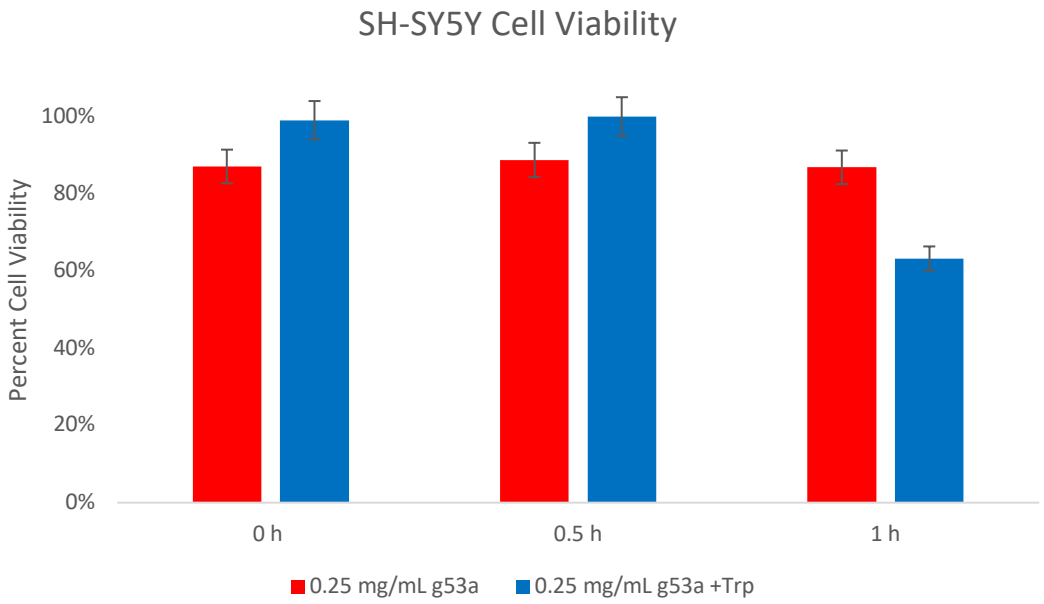

Figure 3.8 MTT assay graphical results of G53A TTR (0.25 mg/mL) mammalian cell viability in the presence and absence of trypsin

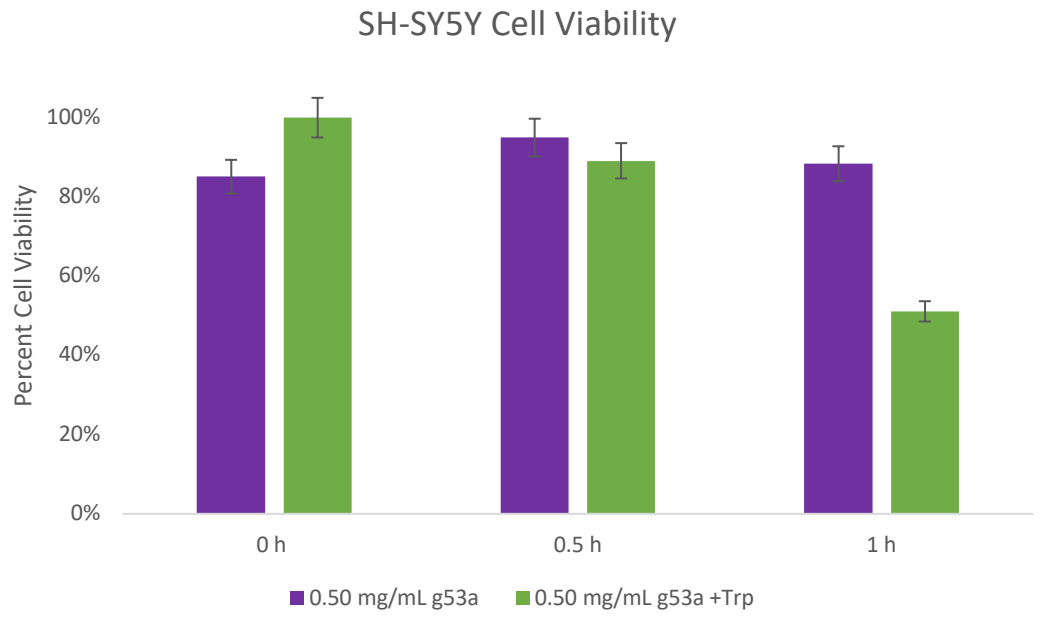

Figure 3.9 MTT assay graphical results of G53A TTR (0.50 mg/mL) mammalian cell viability in the presence and absence of trypsin

Chapter 4: Discussion and Conclusion

It was previously demonstrated that proteolytic cleavage of the peptide bond Lys48-Thr49 of the CD loop in TTR mutants S52P and E51_S52dup promoted aggregation, variants associated with neurodegenerative diseases. Different amyloidogenic phenotypes, including amyloid consisting of full-length or C-terminal 49 – 127 fragment TTR, have been detected *in vivo*, suggesting distinct aggregation mechanisms. In this study, the misfolding and aggregation mechanism of another TTR variant associated with amyloidosis, G53A, was investigated at physiological conditions in the presence and absence of proteolytic agent, trypsin.

In a previous study, it was stated that G53A TTR tetramers gradually dissociate to monomers and thus form oligomers at physiological conditions.[5] However, when incubating G53A TTR at physiological pH and at low temperature (4 °C), studies of the early-stage of the aggregation cascade were possible as a result of slowing down aggregation kinetics.[5] Oligomers were the dominating species after 2 d incubation, as demonstrated by SEC analyses and TEM images.[5] In this study TEM was utilized to compare different cytotoxic agents formed at the earlier stage of fragmented and full-length G53A TTR aggregation under physiological conditions. In contrast to results generated when incubating G53A TTR at the neutral pH and at 4 °C, oligomeric species were present in clusters after 2 h incubation at physiological conditions (Figure 3.1a). Even more oligomeric clusters were noticed when G53A TTR was incubated with trypsin (Figure 3.1b), suggesting aggregation is promoted when G53A TTR experiences a proteolytic cleavage. However, the morphology of the oligomers formed in the absence

and presence of trypsin was similar (Figure 3.2), implying a similar misfolding and aggregation pathway. G53A TTR structural changes were monitored with CD. The generated spectra for G53A TTR in the presence and absence of trypsin are not significantly different (Figure 3.5-3.6). Both the β-characteristic positive and negative bands are present in the same wavelength for both G53A TTR samples, with the protein experiencing slightly more spectrum fluctuations in the presence of trypsin. Congruent with the TEM results, the CD findings suggest cleaved and un-cleaved G53A TTR undergo similar misfolding and aggregation.

Direct aggregation kinetic studies were achieved for fragmented and full-length G53A TTR by monitoring optical density (Figure 3.3). Low turbidity was experienced by G53A TTR in the absence of trypsin. However, turbidity notably increased in the presence of trypsin as a result of more precipitates or insoluble amyloidogenic species forming in solution. The findings suggest protein aggregates form quicker in solution when G53A TTR was subject to digestion by trypsin. To confirm the presence of amyloidogenic species in solution, the ThT fluorescence signal of the variant in the presence and absence of trypsin was examined (Figure 3.4). At 5 h incubation, a much greater ThT enhancement was observed for the TTR variant in the presence of trypsin, implying amyloid was present and more abundant than when TTR variant was un-cleaved. Aggregation is promoted when G53A TTR is cleaved. To investigate the amyloid molecular structure of G53A TTR formed in the presence and absence of trypsin, FT-IR was employed. After 14 d incubation, to ensure amyloid was the dominating species, FT-IR profiles of both G53A TTR samples were strikingly similar. The findings suggest amyloid with similar β-structure are formed by cleaved and full-length G53A TTR

misfolding. The results further support the hypothesis that fragmented and full-length G53A TTR misfold and aggregate via a similar mechanism.

It has been proposed the oligomers, the earliest intermediates of the amyloidogenic cascade, are real cytotoxic agents. TEM determined the oligomers formed are of same morphology, implying their toxic effects are similar. The differences in toxicity of the G53A TTR oligomers produced in the absence and presence of trypsin was determined using employing the MTT assay (Figure 3.7-3.8) Mammalian cell viability notably decreased over time when treated with cleaved G53A TTR as opposed to treatment with full-length TTR. The findings suggest proteolytic cleavage speeds up oligomerization, rendering G53A TTR more toxic to cells.

References

1. Ashraf, G., Greig, N., Khan, T., Hassan, I., Tabrez, S., Shakil, S., & Kamal, M. (2014). Protein Misfolding and Aggregation in Alzheimer's Disease and Type 2 Diabetes Mellitus. CNS Neurol Disord Drug Targets, 13(7), 1280-1293.
2. Buxbaum, J. N. & Ruberg, F. L. (2017). Transthyretin V122I (pV142I)* cardiac amyloidosis: an age-dependent autosomal dominant cardiomyopathy too common to be overlooked as a cause of significant heart disease in elderly African Americans. Genetics in Medicine, 19, 733-742.
3. Connors, L. H., Lim, A., Prokaeva, T., Roskens, V. A., & Costello, C. E. (2003). Tabulation of human transthyretin (TTR) variants. Amyloid, 10(3), 160-184.
4. CSIR NET Life science study material (2018). Protein structure- primary, secondary, tertiary and quarternary structure. Retrieved from http://easylifescienceworld.com/levels-of-organization-in-proteins/.
5. Dasari et al (2019). Transthyretin aggregation pathway toward the formation of distinct cytotoxic oligomers. Sci Rep, 9(33), 1-10.
6. Department of Biology at University of York (n.d.). Circular Dichroism Spectrophotometry. Retrieved from https://www.york.ac.uk/biology/technology-facility/molecular-interactions/mi-equipment/mi-dichromator/.
7. Eisenberg, D., & Jucker, M. (2012). The Amyloid State of Proteins in Human Diseases. Cell, 148(6), 1188-1203.
8. Fandrich, M. (2012). Oligomeric Intermediates in Amyloid Formation: Structure Determination and Mechanisms of Toxicity. Journal of Molecular Biology, 421(4-5), 427-440.
9. Gertz et al (2015). Diagnosis, Prognosis, and Therapy of Transthyretin Amyloidosis. Journal of the American College of Cardiology, 66(21), 2451-2466.
10. Jacobson, D. R., Pastore, R. D., Yaghoubian, R., Kane, I., Gallo, G., Buck, F. S., & Buxbaum, J. N. (1997). Variant-Sequence Transthyretin (Isoleucine 122) in Late-Onset Cardiac Amyloidosis in Black Americans. New England Journal of Med. 336(7), 466-473.

11. João, M., & Saraiva, M. (1995). Transthyretin mutations in health and disease. Human Mutation, 5(3), 191-196.
12. Klimtchuk et al (2018). Unusual duplication mutation in a surface loop of human transthyretin leads to an aggressive drug-resistant amyloid disease. Proceedings of the National Academy of Sciences, 115(28), E6428-E6436.
13. Kumar, S., & Udgaonkar, J. B. (2010). Mechanisms of amyloid fibril formation by proteins. Current Science, 98(5), 639-656.
14. Kumar, S., & Walter, J. (2011). Phosphorylation of amyloid beta (Aβ) peptides – A trigger for formation of toxic aggregates in Alzheimer's disease. Aging, 3(8), 803–812.
15. Langel et al (2010). *Introduction to peptides and proteins*. Boca Raton, FL: Taylor & Francis.
16. Leach, B. I., Zhang, X., Kelly, J. W., Dyson, H. J., & Wright, P. E. (2018). NMR Measurements Reveal the Structural Basis of Transthyretin Destabilization by Pathogenic Mutations. Biochemistry, 57(30), 4421-4430.
17. Lim, K. H., Dyson, H. J., Kelly, J. W., & Wright, P. E. (2013). Localized Structural Fluctuations Promote Amyloidogenic Conformations in Transthyretin. Journal of Molecular Biology, 425(6), 977-988.
18. Lim, K. H., Dasari, A. K. R., Hung, I., Gan, Z., Kelly, J. W., Wright, P. E., & Wemmer, D. E. (2016). Solid-State NMR Studies Reveal Native-like β-Sheet Structures in Transthyretin Amyloid. Biochemistry, 55(37) 5272-5278.
19. Lim, K. H., Dasari, A. K. R., Ma, R., Hung, I., Gan, Z., Kelly, J. W., & Fitzgerald, M. C. (2017). Pathogenic Mutations Induce Partial Structural Changes in the Native β-Sheet Structure of Transthyretin and Accelerate Aggregation. Biochemistry, 56(36), 4808-4818.
20. Mahler, H.-C., Friess, W., Grauschopf, U., & Kiese, S. (2009). Protein aggregation: Pathways, induction factors and analysis. Journal of Pharmaceutical Sciences, 98(9), 2909-2934.
21. Mangione et al (2014). Proteolytic cleavage of Ser52Pro variant transthyretin triggers its amyloid fibrillogenesis. Proceedings of the National Academy of Sciences, 111(4), 1539–1544.

22. Mangione et al (2018). Plasminogen activation triggers transthyretin amyloidogenesis in vitro. Journal of Molecular Biology, 293(37), 14192-14199.
23. Nickla, H., & Klug, W. S. (2012). *Concepts of genetics* (10th edition). San Francisco, CA: Benjamin Cummings.
24. Protein Data Bank in Europe (n.d.). Crystal structure of the highly amyloidogenic transthyretin mutant TTR G53S/E54D/L55S- heated protein. Retrieved from https://www.ebi.ac.uk/pdbe/entry/pdb/2qel/analysis.
25. Ramirez-Alvarado, M., Kelly, J. W., & Dobson, C. M. (2010). *Protein misfolding diseases: current and emerging principles and therapies*. Hoboken, NJ: John Wiley & Sons.
26. Singh, S., & Joshi, N. (2019). *Pathology, prevention and therapeutics of neurodegenerative disease.* Gateway East, Singapore: Springer Nature.
27. Sun, X., Dyson, H. J., & Wright, P. E. (2018). Kinetic analysis of the multistep aggregation pathway of human transthyretin. Proc Natl Acad Sci, 115(27), E6201-E6208.
28. Thylén, C., Wahlqvist, J., Haettner, E., Sandgren, O., Holmgren, G., & Lundgren, E. (1993). Modifications of transthyretin in amyloid fibrils: analysis of amyloid from homozygous and heterozygous individuals with the Met30 mutation. The EMBO Journal, 12(2), 743–748.
29. Wolfe, M. S. (2018). *The molecular and cellular basis of neurodegenerative diseases: underlying mechanisms*. London, England, UK: Elsevier/Academic Press.
30. Wilson, K., & Walker, J. (2010). *Principles and techniques of biochemistry and molecular biology* (7th ed.). Cambridge, NY: Cambridge Univ. Press.